Limiting Step Involved in the Thermal Growth of Silicon Oxide Films on Silicon Carbide

I. C. Vickridge, I. Trimaille, J.-J. Ganem, and S. Rigo
Groupe de Physique des Solides, Universités de Paris 6 et 7, UMR 7558 du CNRS, 2 Place Jussieu, 75251, Paris, France

C. Radtke and I. J. R. Baumvol
Instituto de Física, UFRGS, Avenida Bento Gonçalves 9500, Porto Alegre, RS, Brazil, 91509-900

F. C. Stedile*
Instituto de Química, UFRGS, Avenida Bento Gonçalves 9500, Porto Alegre, RS, Brazil, 91509-900
(Received 19 July 2002; published 27 November 2002)

Thermal growth of silicon oxide films on silicon carbide in O_2 was investigated using oxygen isotopic substitution and narrow resonance nuclear reaction profiling. This investigation was carried out in parallel with the thermal growth of silicon oxide films on Si. Results demonstrate that the limiting steps of the thermal oxide growth are different in these two semiconductors, being diffusion limited in the case of Si and reaction limited in the case of SiC. This fact renders the growth kinetics of SiO_2 on SiC very sensitive to the reactivity of the interface region, whose compositional and structural changes can affect the electrical properties of the structure.

DOI: 10.1103/PhysRevLett.89.256102 PACS numbers: 81.65.Mq, 61.82.Fk, 68.35.Fx, 77.55.+f

In semiconductor device applications involving high power, frequency, voltage, and/or temperature, Si use is limited by its physical properties. An example is the relative narrow band gap (1.1 eV) that prevents Si devices from operating at high temperatures. The polar crystal silicon carbide (SiC) appears to be the wide band-gap material of choice since besides the wider gap (2.9 eV for the 6H polytype) SiC has other desired properties such as high thermal conductivity, breakdown voltage, and saturated electron drift velocity. It is also the only known compound semiconductor on which SiO_2 can be grown thermally. On the other hand, the properties of the SiO_2/SiC interface lead to electrical characteristics worse than those of SiO_2/Si, while the scatter of the available data [1] suggests poor interface control. Investigations of the thermal oxide film on SiC in its different regions have been pursued [2–7], indicating that in the surface and bulk regions the oxide is similar to that grown on Si [4,8,9], that the interface is less abrupt [5,10], and that incompletely oxidized C or Si are found near the interface [2,3,6,7,11–14]. However, a thorough understanding of the phenomena taking place during the thermal growth of SiO_2 on SiC is still missing.

Growth of SiO_2 on SiC is much slower than on Si, presenting more scattered data [15–17] and differences along the polar directions [$(000\underline{1})$ and (0001) in the hexagonal polytypes]. Several authors have tried to model the kinetics of the thermal growth of SiO_2 on SiC [15,17,18], mostly within the framework of the Deal and Grove model [19], which satisfactorily describes the thermal growth of SiO_2 on Si in dry O_2 for oxide thicknesses above 20–30 nm. This model is based on a stationary flux of O_2, the only mobile species, across the growing oxide and on reaction with Si to form SiO_2 only at an abrupt interface. These efforts were curve fittings which did not consider the reaction mechanisms and limiting steps characteristic of the SiO_2/SiC system. The elucidation of the oxidation mechanisms—identification of the limiting steps and the mobile species and how they are transported during oxide thermal growth—is necessary to develop an oxidation model for SiC allowing prediction and control of the oxide film properties (including electrical) based on oxidation parameters.

In the present work oxygen isotopic substitution and narrow resonance nuclear reaction profiling (NRP) [20] were used to follow oxygen atomic transport during oxide thermal growth. By starting oxidation of SiC wafers in natural O_2 ($^{16}O_2$) and then substituting it by ^{18}O enriched O_2 ($^{18}O_2$) one can follow where and how much the newly incorporated atoms from the gas phase fix themselves. NRP was used to profile these ^{18}O atoms nondestructively with nanometric resolution. Si wafers were submitted to identical oxidation procedures and analysis. From previous works it is known that in the oxide thickness range of the present work the $^{16}O_2/^{18}O_2$ oxidation sequence leads to the incorporation of ^{18}O in near surface and near-interface regions for both SiC [17,21,22] and Si [20,23,24] indicating that the oxidant species is mobile in both cases. In the case of Si oxidation, ^{18}O fixation near the surface is due to ^{16}O-^{18}O exchange mediated by defects existing in this region [23]. ^{18}O fixation near the interface is due to interstitial diffusion of O_2 across the growing oxide without interacting with it and reaction with Si at the interface, forming SiO_2, while Si was shown to be practically immobile being absent in its nonoxidized form away from the interface region [25]. However, it has not been proven that O_2 is the only mobile species in the case of SiC, since both Si and C could also be mobile and take part in the oxide growth process in the

 0031-9007/02/89(25)/256102(4)$20.00 © 2002 The American Physical Society

near-interface reactive layer, which is apparently much wider in SiC than in Si. The thermal growth rate of SiO_2 on SiC is up to 1 order of magnitude lower than that of Si. If we consider that thermally grown oxides on these two semiconductors are alike, except for the near-interface region, this difference in growth rate must be ascribed to differences in the oxide/semiconductor interface region, which is where reaction takes place. Thermal growth of SiO_2 on Si to thicknesses > 50 nm (SiO_2 thickness of interest in the present SiC technology) is governed by diffusion of the oxidant species [19]. However, the growth rate of SiO_2 on SiC suggests a reaction limited process. In the following we present the strategy used here to test this hypothesis.

6H-SiC and Si (001) wafers were submitted to different sequential oxidation processes in natural O_2 (< 1 ppm of water, termed $^{16}O_2$) and then in ^{18}O enriched (97%) O_2 (termed $^{18}O_2$) under static pressure. Excitation curves of the $^{18}O(p, \alpha)^{15}N$ nuclear reaction around the resonance at 151 keV [20] were obtained for each sample and simulated using the SPACES code [26], from which ^{18}O profiles were extracted. A depth resolution of $\sim$0.7 nm is obtained near the oxide surface.

One set of SiC samples was thermally oxidized in a single batch in $^{16}O_2$ (45 h, 1100 °C, 100 mbar), etched in a HF water solution (1 nm/s etching rate) for different times (1, 10, 20, and 30 s) and then all oxidized in $^{18}O_2$ (1 h, 1100 °C, 100 mbar). The aim was to generate different thicknesses of $Si^{16}O_2$ (due to the different etching times) that the oxidizing species would traverse during the second oxidation step in $^{18}O_2$, but identical $Si^{16}O_2/Si$ interfaces where it would react to form new oxide, since HF attacked only the external surfaces. The 1 s etching step was performed in order to ensure the same type of SiO_2/air interface to all samples. In parallel, Si wafer samples were oxidized in $^{16}O_2$ (8 h, 1100 °C, 100 mbar), etched in the same HF solution for different times (1, 30, 40, and 70 s) and then submitted to $^{18}O_2$ (1 h, 1100 °C, 100 mbar). ^{18}O excitation curves are shown in Fig. 1 for SiC ($000\underline{1}$) (C-face, top) and Si (001) (bottom). In the respective insets are the profiles used to simulate the excitation curves. A sketch of the HF-etching idea employed to generate different $Si^{16}O_2$ thicknesses and identical interfaces is shown in the top of the figure. All profiles exhibit an ^{18}O rich region erfc-like at the sample surface and another one, boxlike, at the oxide/semiconductor interface region. The final thickness of the oxides grown on SiC ($000\underline{1}$) are approximately 52, 65, 76, and 86 nm, while, on Si (001), they are 106, 134, 140, and 166 nm.

When comparing the results from SiC and Si samples two differences are apparent: (i) from the analysis of the excitation curves, the amount of ^{18}O fixed at the interface region is essentially the same in all SiC ($000\underline{1}$) samples (950 ± 30 areal units), while in the case of Si samples it increases with the etching time (3660, 4300, 6250, 6950 areal units); (ii) from the profiles, the percentage of ^{18}O fixed in the interface region (see heights of the boxes in the insets of Fig. 1) on SiC ($000\underline{1}$) is less than the isotopic enrichment of the $^{18}O_2$ gas (97%) while it is equal to the isotopic enrichment in the case of Si samples, evidencing that in this last case the amount of ^{18}O incorporated in the interface region formed stoichiometric $Si^{18}O_2$. This result is also observed when comparing the heights of the surface and interface peaks in the excitation curves and corroborates previous findings [21,22]. Only the excitation curve corresponding to the thinnest

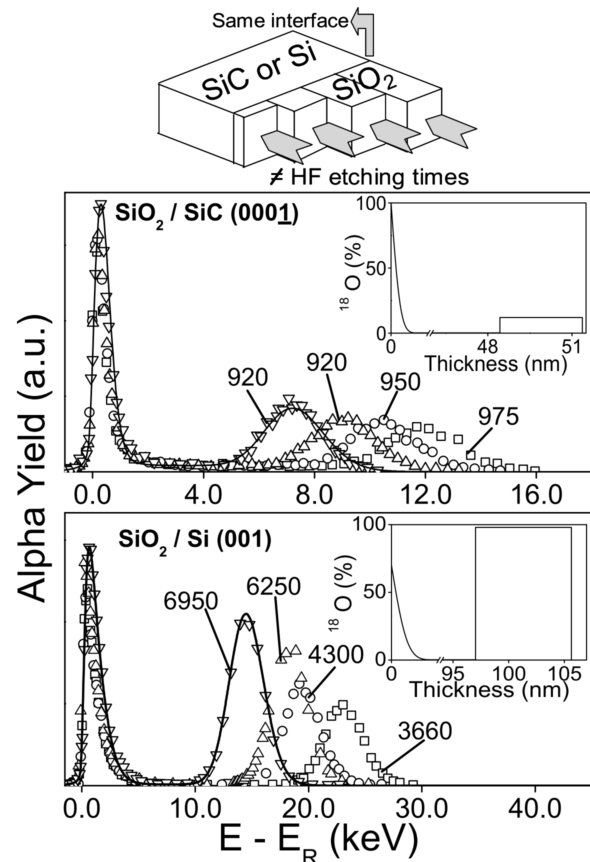

FIG. 1. Experimental excitation curves (symbols) of the $^{18}O(p, \alpha)^{15}N$ nuclear reaction around the resonance at 151 keV and the corresponding simulations (lines) obtained using SPACES for silicon oxide films thermally grown on SiC ($000\underline{1}$) (top) and on Si (bottom). Symbols in the upper graph are related to the $Si^{16}O_2$/SiC ($000\underline{1}$) samples etched for 1 (□), 10 (○), 20 (△), and 30 s (▽). Symbols in bottom graph are related to the $Si^{16}O_2$/Si samples etched for 1 (□), 30 (○), 40 (△), and 70 s (▽). The area of each interfacial peak is indicated in the respective excitation curve. A sample tilt of 30° was used during analyses. ^{18}O profiles used for the simulations of excitation curves are shown in the respective insets. Concentration is normalized to O in stoichiometric SiO_2. A sketch of the HF-etching idea employed to generate different $Si^{16}O_2$ thicknesses and identical interfaces is shown in the top of the figure. a.u. stands for arbitrary units.

oxide on SiC (000$\bar{1}$) is presented with its simulation because straggling prevents an accurate profile determination in the other samples. However, these excitation curves could be well fitted using a similar profile to the one shown in the inset, only its starting position being deeper in the sample, corroborating the result obtained analyzing the areas under the excitation curves.

The results from Si samples confirm the idea that the oxide thermal growth process is limited by diffusion of the oxidant species in the existing SiO_2 layer, since for thicker $Si^{16}O_2$ films the amount of newly formed $Si^{18}O_2$ at the interface is smaller. On the contrary, for SiC (000$\bar{1}$), results corroborate the idea that the oxide thermal growth process is limited by reaction of the oxidant species in the interface region, since the amount of newly formed $Si^{18}O_2$ at the interface did not depend on the thickness of $Si^{16}O_2$ films that the $^{18}O_2$ had to traverse before reaching the SiC/SiO_2 interface. As the $^{16}O_2$ oxidation conditions were identical for all SiC samples, very similar interfaces (with respect to composition, chemical environment, structure, etc.) must have been created, yielding similar conditions for reaction to occur and thus similar interfacial oxygen uptake in SiC (000$\bar{1}$) samples. In Si samples the O_2 molecules diffuse through the oxide, reach the oxide/Si abrupt interface, and there they react forming new $Si^{18}O_2$, a behavior predicted a long time ago [19]. On the other hand, for SiC the behavior can be explained by an oxide thermal growth mechanism in which the oxidant species reacts in a region near (and including) the oxide/Si interface and not at an abrupt interface as in the case of Si samples. This interface cannot be wider than 15 nm, according to previous results [22]. In this near-interface reactive region [2,3,6,7,11–14] carbon and/or excess silicon (from SiC not completely oxidized or from Si interstitials injected as a result of SiC oxidation) may also be present. The mobility of lattice oxygen could also be responsible for this phenomenon, but it has been ruled out [21] by previous analyses of samples oxidized in the $^{16}O_2/^{18}O_2/^{16}O_2$ gas sequence.

The magnitudes and shapes of the ^{18}O profile found in near surface regions of SiC samples were practically superposable to those of thermal oxides formed on Si (100) under identical conditions. These facts, together with the absence of ^{18}O above its natural abundance of 0.2% in the oxides bulk (indicating that O_2 diffuses without interacting with silica in this region), are further demonstrations of the structural and compositional similarities [1,4,9] between the surface and bulk regions of thermally grown silica films on SiC and on Si, supporting the assumption that the diffusion coefficients of the oxidant species should be similar in both cases.

Thus, we have an evidence that thermal growth of SiO_2 films on SiC is limited by reaction in the near-interface region, while on Si it is diffusion limited. A second set of samples was oxidized for variable oxidation times in $^{16}O_2$ (16, 26, 35, or 45 h at 1100 °C and 100 mbar), etched in the same HF solution for 1 s in all cases, also to ensure the same type of SiO_2/air interface to all samples, and oxidized in $^{18}O_2$ (1 h, 1100 °C, 100 mbar). In parallel, Si wafer samples were oxidized for different times in $^{16}O_2$ (26 or 45 h at 1100 °C and 100 mbar), etched in the same HF solution for 1 s and then oxidized in $^{18}O_2$ (1 h, 1100 °C, 100 mbar). The final thicknesses of the oxides grown on SiC (000$\bar{1}$) are approximately 34, 50, 59, and 75 nm, while, on Si (001), they are 138 and 184 nm. These values are in a range comparable to those of the first set. ^{18}O excitation curves of all samples are shown in Fig. 2. The results for SiO_2/Si exhibit the same trend as in Fig. 1, corroborating the idea of a diffusion limited process. The percentage of ^{18}O fixed in the interface region is equal to the isotopic enrichment of the O_2 gas in the case of SiO_2/Si, while it is smaller than the isotopic enrichment level in the case of SiO_2/SiC. Furthermore, in the case of the present study the amount of ^{18}O fixed in the interface region is seen to decrease in (000$\bar{1}$) face samples (910, 670, 640, 630 areal units) with the increase of the oxidation time in $^{16}O_2$, indicating different reaction rates in this region. A possible consequence of great impact is the dependence of electrical characteristics of the SiO_2/SiC interface on the oxidation parameters.

In summary, based on the present findings we can distinguish between the limiting processes involved in the thermal growth of silicon oxide films on SiC and on Si. While oxide growth on Si is governed by diffusion of the oxidant species through the oxide layer, growth on SiC is limited by reaction in the near-interface region. We observed that the reaction rate in the near-interface regions and therefore the instantaneous oxide growth rate of SiO_2 on SiC was modified in the case of first oxidations of different durations. Discrepancies among kinetics and electrical characterization data in the literature could be explained taking this idea into account. The similar erfc-like profiles found at the surface regions of all films and the absence of ^{18}O newly incorporated in the bulk of the oxides grown on SiC and on Si support the idea, already proposed in previous works, that in these two regions the oxides formed are similar. On the other hand, in the oxide/semiconductor interface region the ^{18}O profiles are similar in shape (boxlike) but differ in area and in the maximum amount of ^{18}O incorporated, evidencing a lower reaction rate and an extended reaction region, in the case of SiC samples, where both oxygen isotopes (^{18}O and ^{16}O) may be present as well as C and/or excess Si. It is worth mentioning that the conclusions obtained here for the C-face are also valid for the Si-face, which results (not shown here) support the same reasoning.

In order to further understand the thermal growth mechanisms of SiO_2 films on SiC and to relate them to those of Si we are currently modeling the thermal growth of SiO_2 films on SiC in O_2 using a reaction-diffusion approach, but to accomplish that, more information is

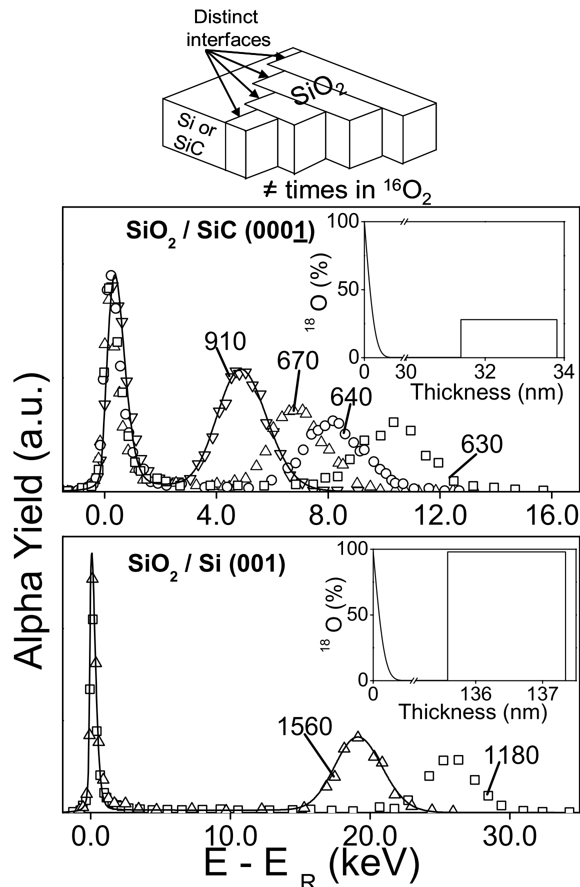

FIG. 2. Experimental excitation curves (symbols) for the $^{18}O(p, \alpha)^{15}N$ nuclear reaction around the resonance at 151 keV and the corresponding simulations (lines) obtained using SPACES for silicon oxide films thermally grown on SiC (000$\underline{1}$) (top) and on Si (bottom). Symbols in the upper graph are related to the $Si^{16}O_2$/SiC (000$\underline{1}$) samples grown for 45 (□), 35 (○), 26 (△), and 16 h (▽), the other oxidation parameters being kept fixed. In the bottom graph, symbols were used to represent the data obtained from the oxide/Si samples oxidized first in $^{16}O_2$ for 45 (□) and 26 h (△), the other oxidation parameters being kept fixed. The area of each interfacial peak is indicated in the respective excitation curve. A sample tilt of 30° was used during analyses. The ^{18}O profiles used for the simulations of samples on SiC and on Si are shown in the respective insets. Concentration is normalized to O in stoichiometric SiO_2. In the top of the figure there is a sketch of the idea of different $^{16}O_2$ oxidation times employed to generate different $Si^{16}O_2$ thicknesses and eventually different interfaces. a.u. stands for arbitrary units.

required on the extended reactive zone in the near-interface region where growth takes place, especially on the nature of the mobile species and the specific kind of defect present in this region. In order to investigate that, we are determining the dependence of the phenomena described here on the gas pressure during the second oxidation step (in $^{18}O_2$) as well as on the oxidation time in $^{18}O_2$. Experiments performed in a symmetric gas sequence $^{18}O_2/^{16}O_2$ are also in progress aiming at confirming the presence of oxygen from the first oxidation step in the reactive region at the interface. Finally, Si isotopic substitution experiments are on course to clarify the injection of interstitial Si in the near-interface region.

This work was partially supported by CNRS, CNPq, PADCT, and FAPERGS.

---

*Electronic address: fernanda@iq.ufrgs.br

[1] C. Raynaud, J. Non-Cryst. Solids **280**, 1 (2001).
[2] C. Virojanadara and L. I. Johansson, Surf. Sci. **472**, L145 (2001).
[3] K. C. Chang, N. T. Nuhfer, L. M. Porter, and Q. Wahab, Appl. Phys. Lett. **77**, 2186 (2000).
[4] M. B. Johnson, M. E. Zvanut, and O. Richardson, J. Electron. Mater. **29**, 368 (2000).
[5] G. G. Jernigan, R. E. Stahlbush, and N. S. Saks, Appl. Phys. Lett. **77**, 1437 (2000).
[6] C. Onneby and C. G. Pantano, J. Vac. Sci. Technol. A **15**, 1597 (1997).
[7] B. Hornetz, H. J. Michel, and J. Halbritter, J. Mater. Res. **9**, 3088 (1994).
[8] V. V. Afanas'ev, Microelectron. Eng. **48**, 241 (1999).
[9] K. McDonald, M. B. Huang, R. A. Weller, L. C. Feldman, J. R. Williams, F. C. Stedile, I. J. R. Baumvol, and C. Radtke, Appl. Phys. Lett. **76**, 568 (2000).
[10] F. Amy, P. Soukiassian, Y. K. Hwu, and C. Brylinski, Appl. Phys. Lett. **75**, 3360 (1999).
[11] C. I. Harris and V. V. Afanas'ev, Microelectron. Eng. **36**, 167 (1997).
[12] S. Wang, M. DiVentra, S. G. Kim, and S. T. Pantelides, Phys. Rev. Lett. **86**, 5946 (2001).
[13] F. Amy, P. Soukiassian, Y. K. Hwu, and C. Brylinski, Phys. Rev. B **65**, 165323 (2002).
[14] C. Radtke, I. J. R. Baumvol, J. Morais, and F. C. Stedile, Appl. Phys. Lett. **78**, 3601 (2001).
[15] A. Suzuki, M. Ashida, N. Furui, K. Mameno, and H. Matsunami, Jpn. J. Appl. Phys. **21**, 579 (1982).
[16] A. Rys, N. Singh, and M. Cameron, J. Electrochem. Soc. **142**, 1318 (1995).
[17] Z. Zheng, R. Tressler, and K. Spear, J. Electrochem. Soc. **137**, 2812 (1990).
[18] K. L. Luthra, J. Am. Ceram. Soc. **74**, 1095 (1991).
[19] B. E. Deal and A. S. Grove, J. Appl. Phys. **36**, 3770 (1965).
[20] I. J. R. Baumvol, Surf. Sci. Rep. **36**, 5 (1999).
[21] I. C. Vickridge, J.-J. Ganem, G. Battistig, and E. Szilagyi, Nucl. Instrum. Methods Phys. Res., Sect. B **161**, 462 (2000).
[22] I. C. Vickridge, D. Tromson, I. Trimaille, J.-J. Ganem, E. Szilagyi, and G. Battistig, Nucl. Instrum. Methods Phys. Res., Sect. B **190**, 574 (2002).
[23] I. Trimaille and S. Rigo, Appl. Surf. Sci. **39**, 65 (1989).
[24] C. J. Han and C. R. Helms, J. Electrochem. Soc. **135**, 1824 (1988).
[25] I. J. R. Baumvol, C. Krug, F. C. Stedile, F. Gorris, and W. H. Schulte, Phys. Rev. B **60**, 1492 (1999).
[26] I. C. Vickridge and G. Amsel, Nucl. Instrum. Methods Phys. Res., Sect. B **45**, 6 (1990).